Chemical Research in Toxicology

pubs.acs.org/crt

Article

Heterogeneous Oxidation Products of Fine Particulate Isoprene Epoxydiol-Derived Methyltetrol Sulfates Increase Oxidative Stress and Inflammatory Gene Responses in Human Lung Cells

Faria Khan, Yuzhi Chen, Hadley J. Hartwell, Jin Yan, Ying-Hsuan Lin, Anastasia Freedman, Zhenfa Zhang, Yue Zhang, Andrew T. Lambe, Barbara J. Turpin, Avram Gold, Andrew P. Ault, Rafal Szmigielski,* Rebecca C. Fry,* and Jason D. Surratt*

Cite This: https://doi.org/10.1021/acs.chemrestox.3c00278

Read Online

ABSTRACT: Hydroxyl radical (˙OH)-initiated oxidation of isoprene, the most abundant nonmethane hydrocarbon in the atmosphere, is responsible for substantial amounts of secondary organic aerosol (SOA) within ambient fine particles. Fine particulate 2-methyltetrol sulfate diastereoisomers (2-MTSs) are abundant SOA products formed via acid-catalyzed multiphase chemistry of isoprene-derived epoxydiols with inorganic sulfate aerosols under low-nitric oxide conditions. We recently demonstrated that heterogeneous ˙OH oxidation of particulate 2-MTSs leads to the particle-phase formation of multifunctional organosulfates (OSs). However, it remains uncertain if atmospheric chemical aging of particulate 2-MTSs induces toxic effects within human lung cells. We show that inhibitory concentration-50 (IC_{50}) values decreased from exposure to fine particulate 2-MTSs that were heterogeneously aged for 0 to 22 days by ˙OH, indicating increased particulate toxicity in BEAS-2B lung cells. Lung cells further exhibited concentration-dependent modulation of oxidative stress- and inflammatory-related gene expression. Principal component analysis was carried out on the chemical mixtures and revealed positive correlations between exposure to aged multifunctional OSs and altered expression of targeted genes. Exposure to particulate 2-MTSs alone was associated with an altered expression of antireactive oxygen species (ROS)-related genes (*NQO-1, SOD-2,* and *CAT*) indicative of a response to ROS in the cells. Increased aging of particulate 2-MTSs by ˙OH exposure was associated with an increased expression of glutathione pathway-related genes (*GCLM* and *GCLC*) and an anti-inflammatory gene (*IL-10*).

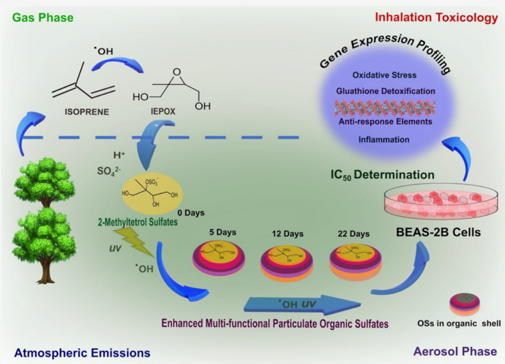

1. INTRODUCTION

Atmospheric fine particulate matter ($PM_{2.5}$, aerodynamic diameter ≤2.5 μm) contributes to poor air quality,[1] climate change,[2] and adverse human health effects.[3] Exposure to $PM_{2.5}$ triggers lung-associated pathologies including asthma, allergy,[4] chronic obstructive pulmonary disease (COPD), bronchitis, emphysema, decreased lung function, and increased cases of lung cancer.[5] Once $PM_{2.5}$ is deposited deep within the lungs, it can cause the induction of inflammatory cascades,[6] including pro-inflammatory cytokines such as interleukin-6 (IL-6), interleukin-8 (IL-8),[7] and C-reactive protein (CRP).[8] These inflammatory cytokines are often associated with endothelial dysfunction, systemic inflammation, and exacerbated myocardial ischemia.[9] In addition to inhalation of $PM_{2.5}$, other gaseous copollutants, such as carbon monoxide, nitrogen oxides (NO_x), ozone (O_3), and sulfur dioxide (SO_2), have been associated with higher instances of cardiopulmonary diseases.[10]

One of the largest $PM_{2.5}$ constituents is often secondary organic aerosol (SOA), formed from the atmospheric oxidation of volatile organic compounds (VOCs).[11] Isoprene is the most abundant nonmethane VOC emitted into Earth's atmosphere (~500 Tg yr^{-1}) and is primarily derived from vegetation.[12] Gaseous isoprene hydroxy hydroperoxides (ISOPOOH) are the most abundant first-generation reaction products (~70% yield) resulting from gas-phase hydroxyl radical (˙OH)-initiated oxidation of isoprene under NO_x-free conditions.[13] ˙OH-mediated oxidation of ISOPOOH predominantly occurs during the daytime and generates a high yield (~75%) of gaseous isoprene epoxydiols (IEPOX).[14] In the presence of inorganic sulfate ($Sulf_{inorg}$) aerosol that is mostly derived from human activities, IEPOX undergoes acid-driven multiphase chemistry to form a variety of low-volatility

Received: September 11, 2023
Revised: September 26, 2023
Accepted: October 4, 2023

organosulfates (OSs) that have been shown to greatly contribute to SOA mass in $PM_{2.5}$ collected from densely forested areas of the Southeastern U.S. and Amazon.[15,16] Particulate methyltetrol sulfates (MTSs) are major products resulting from this multiphase chemistry, with 2-methyltetrol sulfate diastereomers (2-MTSs) being the predominant isomers. 2-MTSs are also the single-most abundant SOA tracers,[17,18] contributing up to 13% of the organic carbon[16,17,19] and up to 15% of the organic mass in $PM_{2.5}$ collected from various U.S. and Amazonian sites.

We recently demonstrated that the heterogeneous $^{\cdot}OH$ oxidation of fine particulate 2-MTSs leads to substantial formation of multifunctional particulate OSs, which are also detected in large quantities within atmospheric $PM_{2.5}$.[20] Increasing the IEPOX-to-$Sulf_{inorg}$ aerosol ratio causes extensive conversion of $Sulf_{inorg}$ to OSs.[21] Climate change will likely cause larger isoprene emissions in the future,[22] while regulatory controls on SO_2 emissions might cause $Sulf_{inorg}$ within $PM_{2.5}$ to primarily exist in OS forms.[21] Hence, systematically examining the early biological changes resulting from inhalation exposures of atmospherically aged particulate OSs (i.e., 2-MTSs), including the multifunctional particulate OS products, is needed in order to aid prediction of acute and long-term exposure responses in humans, especially in a changing atmosphere.

Few studies have focused on airway epithelial cellular responses following exposure to freshly generated isoprene-derived SOA.[23−25] Upper respiratory irritation was demonstrated during previous in vivo studies using mice exposed to gas phase mixtures of isoprene and oxidants (O_3 and NO_2).[26] In other mouse models, Wilkins et al. demonstrated a dependence of the reaction time, relative humidity (RH), and O_3 concentration on airway irritation in mice exposed to isoprene and other organic mixtures.[27] Another study used the dithiothreitol (DTT) assay to measure the oxidative potential (OP) of isoprene-derived SOA generated under low- and high-NO_x conditions. They found higher OP for certain low-NO_x SOA and noted that the OP was comparable to or exceeded that of fresh and aged diesel particles.[28] In an in vitro model using A549 lung cells, exposure to the gas-phase photochemical oxidation products of isoprene and 1,3-butadiene in the presence of NO_x enhanced cytotoxicity and the up-regulation of the *IL-8* gene (a marker of inflammatory response).[29] Similarly, response to nonaged IEPOX-derived SOA induced a less significant reactive oxygen species (ROS)-associated genomic changes when compared with fresh methacrylic acid epoxide (MAE)-derived SOA (a type of isoprene-derived SOA formed in high-NO_x conditions) in BEAS-2B cells.[30,31] *IL-8* and cyclooxygenase 2 (*COX-2*) expression were significantly upregulated at a concentration of 0.067 $\mu g\ cm^{-2}$ following exposure of BEAS-2B cells at an air−liquid interface to photochemically generated isoprene SOA in the presence of initially high-NO_x conditions in acidic $Sulf_{inorg}$ aerosol.[24] We previously reported that 29 micro-RNAs, controlling regulators of inflammatory- and ROS-associated pathways, were differentially expressed in the presence of nonaged IEPOX- and MAE-derived SOA.[32] In both SOA types, significantly altered gene expression was associated with the nuclear factor erythroid-derived 2-like 2 (Nrf2) transcription factor network.[25]

This previous research focused on freshly generated isoprene SOA derived from MAE, IEPOX, and ISOPOOH, which are known isoprene SOA precursors, and provided unique insights into the induction of oxidative stress-related gene expression based on their associated chemical compositions.[31] However, it remains uncertain how atmospheric aging of these fine particle types changes their potential to induce toxicity within human lung cells. In a recent study with viscous, photochemically aged organic aerosol, an increased level of O_2 in the particle interior occurred with decreased viscosity and faster mixing of the particles with carbon-centered radicals (CCR) within the interior of the viscous aerosol.[33] Because 2-MTSs can be viscous and are surface active, it is plausible for 2-MTSs to be present at the aerosol particle surface in the presence of inorganic species.[25] Thus, the accumulation of ROS and CCR may also occur when organic aerosols are enriched in 2-MTSs and have undergone $^{\cdot}OH$-mediated atmospheric aging. RH governs the viscosity of SOA and results in the buildup of ROS within an organic shell.[20,21,33] At low RH, surface MTSs within the shell will be oxidized, and when particles are inhaled in a humid environment such as the interior of the lungs, the higher RH will break down core−shell morphology. Hence, aerosol may no longer be phase separated and become homogeneously mixed within lungs, which may exacerbate negative health outcomes.[33]

In the present study, we hypothesized that the formation of multifunctional OSs from the heterogeneous $^{\cdot}OH$ oxidation of fine particulate 2-MTSs would result in the modification of aerosol physiochemical properties[20] and would also modulate anti-ROS gene expression in lung cells. Using inflammation- and oxidative stress-related genes identified from our previous studies with nonaged isoprene-derived SOA,[23,25] a targeted set of 14 genes was included in the current study. Our results show that these particulate multifunctional OSs, which are seen in $PM_{2.5}$ collected from areas affected by isoprene emissions and acidic $Sulf_{inorg}$ aerosol,[16,34] induce enhanced oxidative stress and inflammatory responses in a human bronchial epithelial lung cell line (BEAS-2B) when compared to nonaged particulate 2-MTSs.

2. EXPERIMENTAL PROCEDURES

2.1. Chemicals and Probes. Sections S1.1 and S1.2 of the Supporting Information (SI) provide the details of chemicals and probes/assays, respectively, included in the current study. As demonstrated in our prior study by Chen et al.,[20] the 2-MTS standard used in this study represent the MTS isomeric mixture in ambient $PM_{2.5}$ samples.

2.2. Generation and Chemical Characterization of Aged Fine Particulate 2-Methyltetrol Sulfates. The experimental setup for generating and collecting aged particles from the heterogeneous $^{\cdot}OH$ oxidation of particulate 2-MTSs is illustrated in Figure S1 and detailed in Section S1.3. Aged particulate 2-MTSs were collected onto 47 mm quartz fiber filters (PALL Corp) at 4 L min^{-1} under each stabilized $^{\cdot}OH$ exposure condition, summarized in Table S1. Blank and sample quartz fiber filters were stored in the dark at −20 °C until extracted in methanol, blown dry, and reconstituted in Milli-Q water to a concentration of 50 mg mL^{-1} (Section S1.3). A 10-μL aliquot of each reconstituted aqueous extract was preserved for analysis by ion chromatography (IC) to quantify $Sulf_{inorg}$ (Section S1.3) and for analysis by hydrophilic interaction liquid chromatography interfaced to electrospray ionization high-resolution quadrupole time-of-flight mass spectrometry operated in negative ion mode (HILIC/(−)ESI-HR-QTOFMS) to quantify OSs and other potential water-soluble SOA constituents. Remaining aqueous extracts were used for biological assays described below. Detailed descriptions for the oxidation flow reactor (OFR), filter processing (or sample workup), and quantitative offline chemical analysis protocols (IC and HILIC/

(−)ESI-HR-QTOFMS) have been previously described and also described in Supporting Information.[17,20,35]

2.3. Cell Viability Analysis. Cell culture details are provided in Section S1.4. Briefly, BEAS-2B bronchial epithelial cells were used for these experiments. A resazurin assay was performed to analyze the percent change in cellular proliferation following treatment with the increasing concentration of heterogeneously oxidized particulate 2-MTSs, compared to an unexposed control. The oxidized 2-MTSs correspond to ambient atmospheric aging of particulates at 0, 5, 12, and 22 days. We analyzed exposure concentrations ranging from 0.01 to 4000 μg mL^{-1} to determine the inhibitory concentration-50 (IC_{50}) for the BEAS-2B cells following 24 and 48 h exposures. For this assay, 10,000 cells well^{-1} were seeded in black-walled 96-well plates and allowed to adhere overnight. Cells were then exposed to aqueous aerosol extracts; after the desired treatment time, the conditioned medium was aspirated, and 100-μL of fresh medium and 20-μL of 0.15 mg mL^{-1} of resazurin were added to each well. Cells were incubated for 3 h, and fluorescence measured using a 560 nm excitation-590 nm emission filter set in a microplate spectrophotometer Promega GloMax (Madison, WI). Results are presented as an average of four independent exposure experiments (biological replicates) with four technical replicates for each exposure concentration.

Final calculations to determine cellular viability percentage were made using the following formula:

$$\begin{aligned}
&\text{Cellular Perecentage of Viability}\\
&\quad = [(\text{Fluorescence of Treated Cells at 560 nm emission}\\
&\quad - \text{Fluorescence of the blank})\\
&\quad /(\text{Fluorescence of Untreated Control Cells at 560}\\
&\quad \text{nm} - \text{Fluorescence of the blank})] \times 100
\end{aligned}$$

where the blank is the well with culture medium and resazurin dye alone, and the untreated control cells were treated with blank filter extracts in DI water.

2.4. Cell Exposure and RNA Extraction. BEAS-2B cells were seeded at 200,000 cells well^{-1} in tissue culture-treated 24-well plates. After allowing them to adhere overnight, cells were then exposed to 0.02, 0.2, and 2 mg mL^{-1} of the four aerosol types (Table S1) as well as a vehicle control (blank filter extract in DI water). We used averaged data from four replicate analyses for each of four exposure samples/concentration for the mRNA gene expression study. Following 24 h exposure, aerosol-treated and control cells were harvested in 350 μL of buffer RLT plus (Qiagen, Valencia CA) and placed in a QIAcube (Qiagen, Valencia CA). Total RNA was extracted using Qiagen's All Prep DNA/RNA/miRNA Universal Kit following the manufacturer's protocol. Quality and quantity of total RNA was determined using NanoDrop-2000c spectrophotometer (ThermoScientific, Waltham, MA, USA), and samples were stored at −80 °C in nuclease-free water until further analysis.

2.5. Gene Expression Analysis. Extracted RNA was used to synthesize 10 μL of 20 ng μL^{-1} cDNA using an Applied Biosystems' High-Capacity cDNA Reverse Transcription Kit, according to the manufacturer's protocol. Two ng μL^{-1} cDNA was the final concentration used for reverse transcription-quantitative polymerase chain reaction (RT-PCR) analysis. cDNA libraries created were stored at −20 °C until analyzed for mRNA expression. Expression changes were evaluated in 14 oxidative stress- and inflammatory-associated genes, with validated SYBR-Green primers obtained from Integrated DNA Technologies (USA). Details of the reverse and forward primers are provided in Section S1.5 and Table S3. Qiagen QuantiTect SYBR Green RT-qPCR Kit was used for gene expression. Analysis and normalization of the NanoString raw data was conducted using nSolver Analysis Software v2.5 (NanoString Technologies). RT-qPCR Ct values were then normalized against the geometric mean of housekeeping gene (*ACTIN*), and fold changes in expression were calculated based on the ΔΔ*Ct* method.[36]

2.6. Data Analysis. The statistical analyses were performed using GraphPad Prism (Version 9.2.0 for Windows, GraphPad Software, La Jolla, CA, U.S., www.graphpad.com). Details of the statistical analysis carried out, including principal component analysis (PCA), in the study are provided in Sections S1.6−S1.11.

3. RESULTS AND DISCUSSION

3.1. Chemical Composition and PCA of Particulate 2-MTSs and Its Aging Products. The relative abundances of specific chemical constituents in the full aerosol mixture for the four different aging times (0, 5, 12, and 22 days of equivalent ·OH exposures) are shown in Figure 1. The details of the

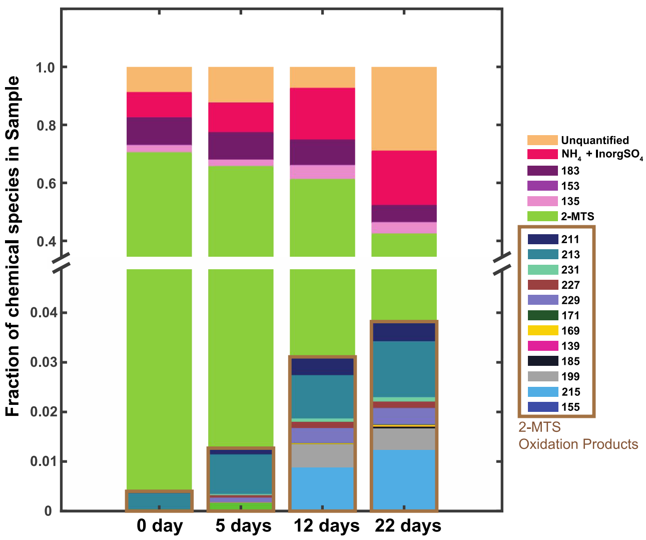

Figure 1. Chemical composition of particulate 2-MTSs under equivalent days of ambient ·OH exposure (0, 5, 12, and 22 days). HILIC/(−)ESI-HR-QTOFMS and IC analyses assessed the chemical changes of particulate 2-MTSs with increased atmospheric chemical aging. The numbers in the legend are the nominal m/z values for monoisotopic deprotonated molecules characterized by HILIC/(−)ESI-HR-QTOFMS. The fractional composition is calculated as the ratio of each identified species (organic and inorganic) to total particulate concentration (measured by SMPS, see Section S1.3).

chemical mechanisms underlying product formation from heterogeneous ·OH oxidation of particulate 2-MTSs shown in Figure 1 have been published elsewhere[20] and will not be fully reiterated here. Briefly, heterogeneous ·OH oxidation of particulate 2-MTSs initiates a cascade of organic peroxy radical ($RO_2^{\cdot}$) reactions in the condensed phase through functionalization and fragmentation.[20] Fragmentation reactions result in the off-gassing of volatile reaction products (e.g., acetic or formic acids) and recycling of particulate $Sulf_{inorg}$, and functionalization reactions lead to formation of low-volatility multifunctional OSs that remain in the particle phase. In this study, we observed substantial compositional changes for the dominant aerosol constituents, including 2-MTSs and $Sulf_{inorg}$, over the course of heterogeneous ·OH oxidation, and we observed OSs that have been previously reported from the heterogeneous ·OH oxidation of 2-MTSs. Oxidation products were detected as deprotonated ions ($[M - H]^-$ ions) at mass-to-charge ratios (m/z) 213 ($C_5H_9O_7S^-$), 211 ($C_5H_7O_7S^-$), 171 ($C_3H_7O_6S^-$), 227 ($C_5H_7O_8S^-$), 229 ($C_5H_9O_8S^-$), 169 ($C_3H_5O_6S^-$), 199 ($C_4H_7O_7S^-$), 155 ($C_2H_3O_6S^-$), 139 ($C_2H_3O_5S^-$), and 185 ($C_3H_5O_7S^-$) measured by HILIC/(−)ESI-HR-QTOFMS.[20] Other $[M - H]^-$ ions measured

https://doi.org/10.1021/acs.chemrestox.3c00278
Chem. Res. Toxicol. XXXX, XXX, XXX−XXX

here included those at m/z 183 ($C_4H_7O_6S^-$), 153 ($C_3H_5O_5S^-$), 135 ($C_5H_{11}O_4^-$) and 197 ($C_5H_9O_6S^-$), which were impurities in the 2-MTS standard present in the nonaged particulate 2-MTS sample.

The full list of observed compounds is summarized in Table S4. Their identities were supported by elemental compositions determined from high-resolution mass fittings and extracted ion chromatograms (EICs) derived from the HILIC/(−)ESI-HR-QTOFMS method; the identified compounds exhibited similar peak shapes and retention times to those previously reported for laboratory-generated and ambient IEPOX-derived SOA (Figure S2).[17,20,37] The fraction labeled "Unquantified" in Figure 1 refers to the residual mass when comparing the sum of HILIC/(−)ESI-HR-QTOFMS and IC quantified tracers with the total mass calculated based on the scanning mobility particulate sizer (SMPS) data (Section S1.3). The residual mass may result from insufficient recovery of some semivolatile organic compounds in filter extraction/sample preparation steps, uncertainties in HILIC/(−)ESI-HR-QTOFMS quantification due to the lack of authentic standards for some compounds, possible changes in aerosol density during aging,[38] or reaction products (e.g., nonsulfated organics) that are not well suited to HILIC/(−)ESI-HR-QTOFMS detection.

3.2. IC_{50} Values of 2-MTS and Its Aging Products in BEAS-2B Cells. The BEAS-2B cells were treated with nonaged and heterogeneously aged 2-MTS aerosol extracts at increasing concentrations ranging from 0.01−4000 μg mL^{-1}. The percent cellular proliferation (Figure S3) was then calculated as a function of blank filter-extract treated cells at 24 and 48 h post exposure relative to the aerosol extracts aged for 0, 5, 12, and 22 days.

Figure 2 shows the dose response curves at 24 h (Figure 2a) and 48 h (Figure 2b) and the corresponding table of IC_{50} values. The IC_{50} values estimated for 24 h exposures at 0, 5, 12, and 22 days of heterogeneous ˙OH oxidation of particulate 2-MTSs were ∼230, 49, 25, and 12 mg mL^{-1}, respectively. At 48 h exposures to extracts from 0, 5, 12, and 22 days of aging, the IC_{50} values were ∼151, 44, 26, and 5 mg mL^{-1}, respectively (Figure 2b). At both exposure time points, the IC_{50} values showed a decreasing trend in cells exposed to increasingly aged particulate 2-MTSs, suggesting that ˙OH mediated aging causes increased particulate toxicity (Figure S3).

In terms of the environmental relevance of the concentrations used, the heterogeneously aged ˙OH oxidation products were in the mg mL^{-1} range. In contrast, ambient atmospheric particulate MTS concentrations reported to date range up to 2.3 μg m^{-3} of 2-MTSs in regions that are heavily impacted by atmospheric oxidation chemistry of isoprene in the presence of anthropogenic-derived $Sulf_{inorg}$.[17,21,34,37,39] Thus, the exposure concentrations used in the lung cells are higher than the environmentally relevant conditions. For the sake of comparison, our previous studies with the α-pinene SOA ozonolysis mixture exhibited IC_{50} values of 912 and 230 μg mL^{-1} in BEAS-2B cells at 24 and 48 h exposures, respectively.[40] Hence, particulate 2-MTSs and their heterogeneous ˙OH oxidation products appear to be less toxic to lung cells than α-pinene-derived SOA particles. Nevertheless, it is important to note that the genomic effects of the 2-MTSs and their heterogeneous ˙OH oxidation products are evident even at elevated exposure concentrations of 0.02 mg mL^{-1} following 24 h exposures. Taken together, future studies should examine the effects of chronic exposure to low-level concentrations of particulate 2-MTSs. Chronic exposure to fine particulate 2-MTSs and their heterogeneous ˙OH oxidation products is important to examine in order to understand the impact on lung cell responses and potential downstream human health effects.

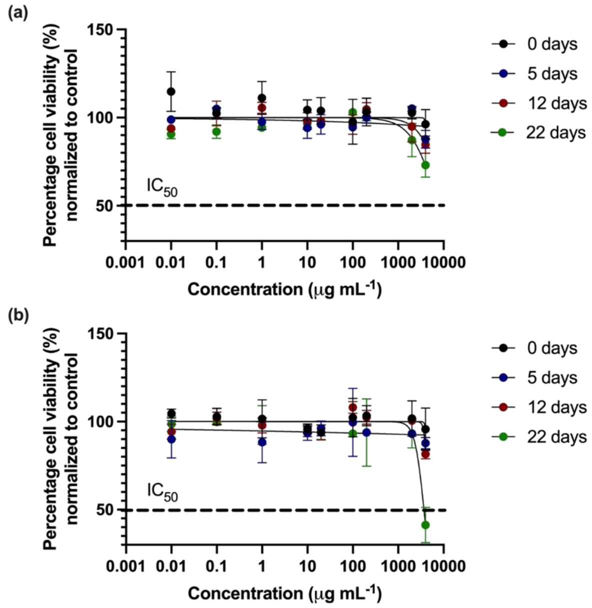

	0 days	5 days	12 days	22 days
24h IC_{50} mg mL^{-1}	290	49	25	12
48h IC_{50} mg mL^{-1}	151	44	25	5.3

Figure 2. Dose−response inhibition curves of 0.01−4000 μg mL^{-1} atmospherically aged aerosol at (a) 24 and (b) 48 h in BEAS-2B cells. Cellular inhibition values were calculated using the resazurin assay relative to untreated-control BEAS-2B cells. The final IC_{50} in mg mL^{-1} were calculated from nonlinear, dose−response curves and estimated using the slope from Hill's equation.

The inverse relationship between the IC_{50} value and atmospheric aging of 2-MTSs implies that the formation of multifunctional OSs by aging mechanisms results in the chemical structures that impair lung cellular growth. In our previous study with α-pinene SOA, ozonolysis of α-pinene created low-volatility particulate organic hydroperoxides that exhibited increased ROS and adversely affected cellular viability.[40] Chowdhury et al.[41] also reported that higher ROS levels mediated cytotoxicity in aged versus fresh SOA samples. In another study with naphthalene-derived secondary organic aerosol (NSOA),[42] altered toxicological profiles were exhibited in the BEAS-2B cells during atmospheric aging. We report a similar decrease in the cell proliferation rate and IC_{50} values with an increased atmospheric aging of particulate 2-MTSs by heterogeneous ˙OH oxidation, thereby highlighting the need to study the aerosol chemical aging processes in the atmosphere to predict the long-term exposure responses.

3.3. Gene Expression Analysis after Exposure of BEAS-2B Cells. BEAS-2B cells were exposed to extracts of fresh and heterogeneously aged aerosol components for 24 h. Gene expression (mRNA) analysis was carried out for 14 genes involved in the antioxidant response, oxidative stress response, glutathione-related signaling pathways, and inflammatory pathways. The ROS-response associated genes have been

https://doi.org/10.1021/acs.chemrestox.3c00278
Chem. Res. Toxicol. XXXX, XXX, XXX−XXX

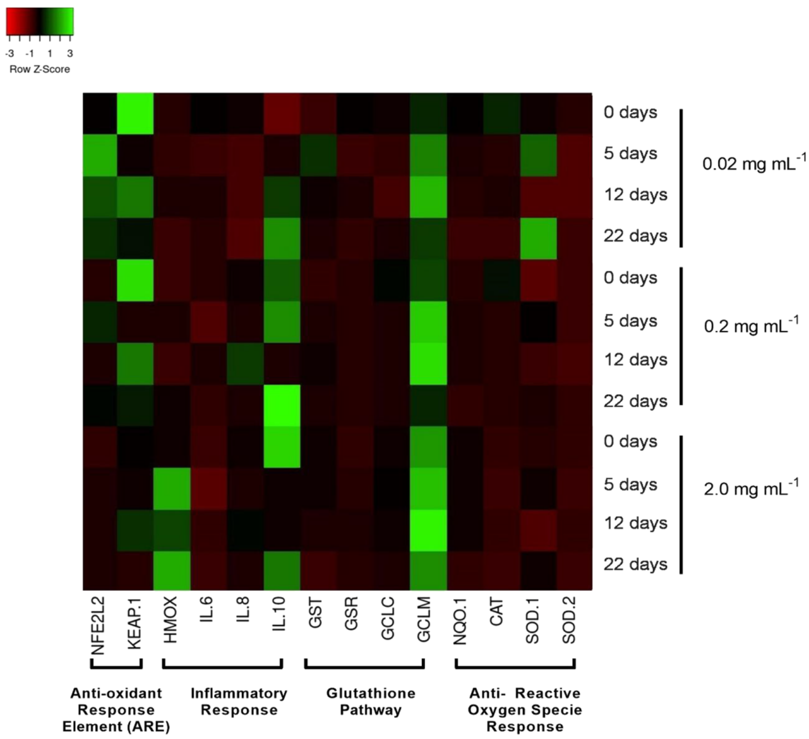

Figure 3. Heat map representing differential gene expression through z-stacked clustering of samples by genes that were upregulated (green) or downregulated (red) following treatment with heterogeneously ·OH-oxidized particulate 2-MTSs at the four atmospherically relevant aging time points shown. This map summarizes the results of three exposure concentrations of 0.02, 0.2, and 2 mg mL^{-1} in BEAS-2B cells. The atmospherically aged 2-MTS aerosol samples (5−22 days of aging) altered the gene expression differentially, implying the role of both increased atmospheric aging and chemical composition as a driver of toxicogenomic changes in current study.

shown to be associated with lung-associated pathologies in previous studies.[23,25,28,53,56,57]

The changes in mRNA expression in comparison to a vehicle control are clustered in a heat map to visualize the effect of atmospheric chemical aging of particulate 2-MTSs (Figure 3). The mean *z*-scores of the gene expression data are displayed, where a positive score (green) represents increased gene expression, while a negative score (red) represents decreased gene expression. Our previous study identified altered expression of 29 oxidative stress- and inflammation-associated genes, enriched for their involvement in the NRF-2 pathway following exposure to the full isoprene-derived SOA mixture.[23,25] The genes included in the present study were from the antioxidant-response elements (ARE) cluster, driven by the transcription factor NF-E2 p45-related factor 2 (Nrf2) and expressed by the *NFE2L2*.[43] The expression of *NFE2L2* is negatively regulated by Kelch-like ECH-associated protein 1 (*KEAP1*), a repressor protein that promotes Nrf-2 degradation.[44] NRF-2 is a key transcription factor in the regulation of the ARE-mediated activation of defensive genes, including *NQO-1*, *GST*, and *HMOX-1*, as well as antioxidant enzymes, cofactors, proteasomes, cytokines, chemokines, and drug transporters;[58] its expression is negatively regulated by *KEAP-1*, once associated secondary genes are switched on.[59]

In this study, we observed downregulation of *NE2FL2* at 0 days of aging (2-MTSs alone) for all the tested concentrations, and upregulation with increased atmospheric aging (Figure 3). 0.02 mg mL^{-1} concentration of 5−12 days of aged particulate 2-MTSs resulted in an ∼5−10-fold increased expression (Figure S4a). *KEAP-1* expression at all concentrations and atmospheric aging time was increased (Figure 3). Significant changes in *KEAP-1* gene expression upon exposure to various atmospherically aged samples was observed; for example, ∼5−15-fold upregulation was observed at 0 days aging, while 5-days aged 2-MTSs only resulted in a ∼3-fold change in expression at all the exposure concentrations studied (Figure S4b). We noted that the expression levels of both *KEAP-1* and *NE2FL2* increased after exposure to aged particulate 2-MTSs. Given their known inverse relationship to each other (i.e., *KEAP-1* serves as a repressor of NRF2), this coexpression at the mRNA level was due to a negative feedback loop that shuts down NRF-2 as soon as oxidative stress is controlled.[59] Since we studied the mRNA-level activation of the ARE cluster,[59] the explanation for this discrepancy is likely at the post-transcriptional level, warranting further studies with our aerosol at the protein level.

The second gene cluster included in the study was from an inflammatory pathway, which included the *HMOX-1, IL-6, IL-8* and *IL-10* genes. Heme oxygenase (HMOX-1) is a protective factor, part of a cluster regulated by ARE-gene, and is associated with anti-inflammatory, antioxidant, and antiproliferative effects.[52,53,54] The 2.0 mg mL^{-1} concentration of aged particulate 2-MTSs resulted in an increased (∼20−80-fold) expression of *HMOX-1*, while significant fold changes in the gene expression were also observed at 0.2 mg mL^{-1} exposure concentration (Figure S5a). *IL-6* and *IL-8* are important pro-inflammatory chemokines that play a role in the genesis and persistence of atmospherically induced airway inflammation.[52,53] *IL-6* exhibited decreased expression at 0.2 and 2.0 mg mL^{-1} exposure concentrations at most aging time points (Figure S5b). *IL-8* was down-regulated at the 0.02 mg mL^{-1} concentration for all aerosol aging points, while up-regulated at the 0.2 and 2.0 mg mL^{-1} exposure concentrations (Figure S5c). *IL-10* exhibited both concentration-dependent and

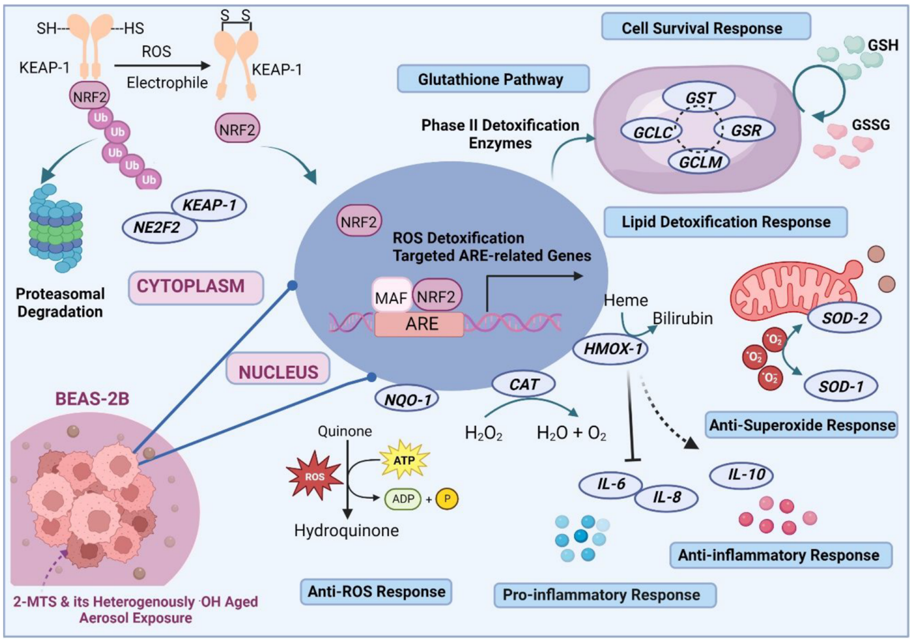

Figure 4. Summary of genes and cellular signaling pathways for the antioxidant, oxidative stress, glutathione detoxification, and inflammatory responses included in this study. Lung cells were exposed to the enhanced multifunctional OS particulate mixtures at 0.02, 0.2, and 2 mg mL^{-1} concentrations to determine the dosage effect on gene expression following exposure at 24 h. The 14 genes included in the study were from Antiresponse Element (ARE) cluster and included some genes encoding for phase II detoxification enzymes, inflammatory cytokines, and anti-ROS enzymes.

atmospheric aging-mediated up-regulation in gene expression, as evident in Figure 3 with ∼20−60-fold increase at 22 days aged aerosol exposure (Figure S5d). The expression of *HMOX-1* in the current study is similar to a prior report on cigarette smoke extract exposure, where the increased expression of *HMOX-1* peaked at 12 h, and returned to baseline levels at 24 h.[63] At higher concentrations, *IL-10* and *HMOX-1* are upregulated, and *IL-6* and *IL-8* are down-regulated; hence, the cellular response shifts from pro-inflammatory to anti-inflammatory signaling.[64] Since *HMOX-1* dysregulation has been reported in several lung pathologies, including asthma[65] and COPD,[66] the chronic exposure studies can establish a role of aged particulate 2-MTSs in inflammation induced adverse lung effects.

Four genes from the glutathione (GSH) detoxification pathway were included, namely, *GCLC, GCLM, GSH,* and *GST*. The GSH pathway encodes for the phase II detoxification enzymes including GSH, an important anti-oxidant protein, involved in the removal of peroxides and xenobiotic electrophiles (Figure 4).[45] The aged particulate 2-MTSs exhibited differential expression when compared to the exposure of nonaged 2-MTSs (Figure 3). *GCLM* expression exhibited up-regulation at all concentrations and exposure conditions (Figures 3 and S6c). *GCLC* expression exhibited up-regulation (∼2−6-fold) after exposure to 0.2 and 2.0 mg mL^{-1} of all four exposure types (Figure S6d). *GSR* was downregulated when exposed to the nonaged 2-MTSs, while at 2.0 mg mL^{-1} concentration, a ∼2−5-fold increase in *GSR* expression was noted when exposed to 5, 12, and 22 days of aged aerosol (Figure S6b). Our results imply conversion of GSSG into GSH as both *GCLC* and *GCLM* expression were upregulated at high exposure concentrations.[46,47] *GST* was upregulated with 0.02 and 0.2 mg mL^{-1} exposure concentrations following exposure to all three aged 2-MTS aerosol. GSH mitigates ROS response and regulates pulmonary inflammation,[45−49] and as observed in previous in vitro studies, *GCLM* up-regulation is observed from diesel exhaust-particulate and cigarette smoke exposures as well as inducing lung inflammation.[67,68] Similarly, *GCLM* and *GCLC* overexpression observed in our study implies GSH accumulation following exposure[45]

Exposure to the $PM_{2.5}$ contributes to ROS production, cellular death, and hyperoxia.[61] Hence, four antioxidant enzymes encoding genes were included in the study, namely, *NQO-1, CAT, SOD-1,* and *SOD-2*. First, the *NQO-1* and *CAT* genes exhibited a concentration-dependent fold change in expression that differed between the exposure types (0−22 days). When exposed to the 2.0 mg mL^{-1} concentration of all exposure types (0, 5, 12, and 22 days), *NQO-1* displayed increased expression (∼3-fold) while *CAT* was downregulated (∼2 fold) (Figures 3, S7a,b). One of the first enzymes contributing to cellular ROS buildup is nicotinamide adenine dinucleotide phosphate (NADPH) dehydrogenase that produces $^{\cdot}O_2^{-\cdot}$.[51] *NQO-1*, the gene encoding for this enzyme, was slightly altered in the current study, along with the *CAT* gene, which encodes for catalase enzyme. *NQO-1* expression was upregulated following exposure to the 2.0 mg mL^{-1} concentration of aged 2-MTSs (Figure 3). A previous COPD study on smokers revealed that catalase was downregulated in bronchiolar epithelial cells, as can be observed in our study as well by our measurement of *CAT*.[61,62]

The anti-ROS response includes superoxide dismutase (SOD) enzyme synthesis, which is involved in the metabolism of superoxide anions. SOD-1 is cytoplasmic while SOD-2 is exclusive to mitochondrial spaces.[50] *SOD-1* was upregulated (∼2−30-fold) when exposed to 5- and 22-days equivalent aged aerosol (Figures 3, S7c) and downregulated (∼1−8-fold) when exposed to 0- and 12-day aged aerosol (Figure S7c). *SOD-2* was downregulated (∼3-fold) following exposure to all 2-MTSs (Figure S7d). The downregulation of *SOD-2* suggests superoxide depletion within 24 h of exposure of particulate 2-MTSs, and as observed in previous studies, decreased synthesis of SOD enzymes occurs through negative feedback mechanism.[60] Our results highlight the altered expression of anti-ROS enzyme-encoding genes within 24 h of exposure, which was significantly altered by the exposure type and concentration.

3.4. Multiple Linear Regression (MLR) Model for Altered Gene Expression. PCA was carried out on four different heterogeneously aged particulate 2-MTS samples (Table S1) to reduce the dimension of the variables. We then performed MLR modeling to understand which of the 14-studied genes exhibited altered expression due to atmospheric aging of particulate 2-MTS.

The biplot of PCA in Figure S8a explains the variance based on the degree of atmospheric aging of samples (along the *x*-axis, PC1) and the variance based on the chemical composition differences (along the *y*-axis, PC2). As shown in Figure S8b, three PC components explained the total variance of 82.37% for PC1 and 12.72% for PC2. Since the values for PC1 could explain the variance greater than 80% (Table S5), we only included PC1 in our current analysis. The MLR model was used to determine the dependence of PC1 on driving changes in the gene expression. As shown in the biplot in Figure S8a, PC1 showed a positive correlation value for 16 of the 18 variance values studied (i.e., $[M-H]^-$ ions at the m/z values measured by HILIC/ESI-HR-QTOFMS), while a negative correlation with 2 variance values (i.e., $[M-H]^-$ ions at m/z 183 and 215, with the latter associated with the 2-MTSs). The 2-MTSs and m/z 183 (main impurity, 10%) were the dominant precursors in the nonaged sample (0 days aging of 2-MTSs),[20] while the remaining chemical components (m/z values) increased due to the heterogeneous $^{\cdot}$OH oxidation of the nonaged samples. Hence, PC1 explains the variance resulting from the aging and helped reduce the chemical components into aged and nonaged chemical products alone. This enabled us to exclude other factors, such as structural or chemical composition dependence, on gene expression. Table S6 summarizes the PC1 scores generated that were analyzed with the gene expression values during MLR analysis.

Table S7 summarizes the results from the MLR modeling, where β_0 (p-value ≤ 0.05) represents the gene expression levels following exposure to nonaged components of particulate 2-MTSs (i.e., m/z 183 and 215). Similarly, β_1 (p-value ≤ 0.05) shows how exposure to m/z values corresponding to the heterogeneous $^{\cdot}$OH oxidation products of particulate 2-MTSs (as well as NH_4^+ + SO_4^{2-}) drove the differential gene expression in the cells. As observed from the results summarized in Table S7, exposure to different concentrations of the four exposure types changed the dependence of gene expression (marked with an asterisk) to PC1. At the 0.02 mg mL^{-1} exposure concentration, *GCLM* exhibited β_0 with p-value of 0.043, while *IL-10* exhibited β_1 with p-value of 0.045. At the 0.2 mg mL^{-1} exposure concentration, *CAT* (β_0 with a p-value of 0.019 and β_1 with a p-value of 0.044), *SOD-2* (β_0 with a p-value of 0.028), *GCLC* (β_0 with a p-value of 0.022), *and IL-10* (β_0 with a p-value of 0.049 and β_1 with a p-value of 0.052) genes exhibited a significant dependence on atmospheric aging. Similarly, at the 2.0 mg mL^{-1} exposure concentration, *NQO-1* (β_0 with p-value of 0.023), *CAT* (β_0 with p-value of 0.003), *SOD-2* (β_0 with p-value of 0.002), *GCLC* (β_0 with p-value of 0.0018), *GCLM* (β_0 with p-value of 0.001 and β_1 with p-value of 0.015), and *IL-6* (β0 with p-value of 0.029) showed dependence on 2-MTSs aging.

MLR results confirm the concentration-dependent effect of aged particulate 2-MTSs on the following genes: *NQO-1*, *CAT*, *GCLC*, *GCLM*, *IL-6*, *IL-10*, and *SOD-2*. Our results show that only 7 of the genes included in the study were differentially regulated when exposed to the increasingly aged particulate 2-MTSs. Note that the heat-map data in Figure 3 shows that exposure to increasingly aged 2-MTSs caused significant changes in the gene expression (*NFE2L2*, *KEAP-1*, *GCLM*, *GCLC*, *SOD-1*, *SOD-2*, *IL-6*, and *IL-10*). Our MLR model was able to predict the dependence on atmospheric aging (i.e., decreased 2-MTSs) in only a few of the genes. The gene pathways included in our study are summarized in Figure 4. As noticed through MLR model, only the genes that regulate the phase II detoxification enzymes[45−49] showed dependence on increased atmospheric aging of the 2MTSs. As explained in the Figure 4, these genes requlate proteins/enzymes involved in cell survival, ROS response, and one gene from anti-inflammatory response (*IL-10*).

In our previous studies,[23,25,30] we reported that the exposure to the full isoprene-derived SOA mixture resulted in altered gene expression within the NRF-2 and oxidative stress pathways (summarized and compared in Table S8). The result from the current study expands on this by including the effect of atmospheric chemical aging on gene expression with corresponding chemical analysis. In a study with gasoline-derived $PM_{2.5}$, the effect of various gasoline components on altering gene expression within BEAS-2B cells was revealed through multivariate PCA.[69] This prior study showed that the aromatic component in the fuel altered gene expression, and hence, the toxicological responses were attributed to a specific chemical type within the exposed $PM_{2.5}$ mixture, while our results link both atmospheric aging and composition as a driver of differential gene expression. Similarly, in a study by Han et al.,[42] NSOA exposed in BEAS-2B cells revealed the effect of carbonyl components as a driver of post-translational toxicology following atmospheric chemical aging. Our study demonstrates that heterogeneous $^{\cdot}$OH oxidation of 2-MTSs, leads to gene expression changes within BEAS-2B cells. The GSH detoxification pathway[61] and anti-inflammatory response genes[55] exhibited significant dependence on aging of particulate 2-MTS. Notably, the expression levels of *NQO-1*, *SOD-2* and *CAT* resulting from exposure to freshly generated 2-MTS particles suggests ROS-induced response within treated cells.

4. CONCLUSIONS

The most significant change in the chemical composition resulting from the $^{\cdot}$OH oxidation of 2-MTSs is the dramatic decrease in the 2-MTS mass fraction from ~80 to ~50% from 0 to 22 days and increased multifunctional OSs formation with the increased atmospheric aging. The yield of low-volatility multifuctional OSs from 2-MTSs was only up to 4% aerosol mass fraction in the 22 days aged samples. However, contributions of the OSs and nonsulfated particle-phase products could be higher owing to the fact that 25% of the aerosol mass reamined unquantified at the molecular level. OSs may be included in this unassigned mass, but this remains uncertain since we lacked authentic standards to quantify the OS products resulting from aging particulate 2-MTSs by HILIC/(−)ESI-HR-QTOFMS; this highlights the need for continued synthesis of critical chemical constituents within

https://doi.org/10.1021/acs.chemrestox.3c00278
Chem. Res. Toxicol. XXXX, XXX, XXX−XXX

$PM_{2.5}$. Previous atmospheric measurements find much higher particulate mass contributions from these multifunctional OSs products in $PM_{2.5}$ than the most aged samples genereated in this work, especially in urban areas impacted by isoprene emissions.[34,70] For example, OSs at m/z 211 ($C_5H_7O_7S^-$) and 213 ($C_5H_9O_7S^-$) are the second and third most abundant OSs, respectively, following 2-MTSs, and their sum contributing ~2% of total particulate OC mass in $PM_{2.5}$ samples collected from Atlanta, GA U.S. in summer.[34] This likely means particulate 2-MTSs can become more aged or accumulate during atmospherically relevant lifetimes (from 2 to 3 weeks) of $PM_{2.5}$ in urban areas due to their low volatilities.[71] The most aged sample that was attainable under our experimental setup (2.85×10^{12} molecules cm^{-3} s $^{\cdot}OH$ exposure) only corresponds to 3−8 equiv aging days in an urban setting with a gas-phase $^{\cdot}OH$ concentration of 4×10^6−1.1×10^7 molecules cm^{-3}.[72] Since it is challenging to generate more aged aerosol samples with our current experimental setup, synthesizing the multifunctional low-volatility OSs products we identified in this study will help to elucidate their individual toxicities in a mixture that is representative of their chemical composition in atmospheric $PM_{2.5}$.

Furthermore, atmospheric aging of particulate 2-MTSs was shown to modulate the expression of genes within pathways under the control of KEAP-1/NRF-2 and inflammatory cluster. The gene expression changes that were observed in relation to nonaged 2-MTS particles included ROS enzymes and genes involved in inflammatory response cascades. The altered expression of enzyme-encoding ROS-responsive genes in the exposed cells indicates increased antioxidant and cellular survival responses. The GSH pathway also exhibited gene upregulation with increased 2-MTSs aging. There is also evidence of gene expression shifts from pro-inflammatory to anti-inflammatory signaling, thereby we conclude heterogeneous $^{\cdot}OH$ oxidation of 2-MTSs drives the IC_{50} and gene expression in the exposed BEAS-2B cells. When comparing the IC_{50} values from this study with our prior data using BEAS-2B cell lines,[40,73] we found that particulate 2-MTSs and their aged particulate products exhibited higher IC_{50} values. Particulate nitrophenols were recently shown by our group to be the most toxic in BEAS-2B cells,[73] followed by α-pinene SOA and then 2-MTSs and its aged particulate products examined in the current study. Future studies using isoprene-SOA should focus on exposure effects at the translational level, as protein changes could be different from mRNA-level changes.[42] Finally, as acute studies carried out in the current study may not elucidate chronic exposure effects of chemically aged particulate 2-MTSs,[74] future research should include in vivo models as these can help better predict the systematic inflammation or irritation in the respiratory system.

■ ASSOCIATED CONTENT

Supporting Information

The Supporting Information is available free of charge at https://pubs.acs.org/doi/10.1021/acs.chemrestox.3c00278.

S1.1−S1.2: Chemicals and probes: the list of chemicals/probes included in the study; S1.3: method for aerosol generation, extraction, and chemical analysis; S1.4: cell culture details; S1.5: primers list for RT-PCR. S1.6−S1.9: IC_{50} calculation, statistical analysis, and heat map details; S1.10−S1.11: methodology for analysis of PCA and MLR; Tables S1−S2: experimental summary for aged 2MTSs and standards used; Table S3: primer sequences for RT-PCR; Table S4: organic compounds in aged 2MTSs; Tables S5−S7: PCA and MLR analysis details; Table S8: previous toxicological studies on similar SOA; Figure S1: PAM reactor experimental setup; Figure S2: HILIC/ESI-HR-QTOFMS EICs of aged 2-MTS aerosol; Figure S3: viability graphs; Figures S4−S7: RT-PCR mRNA expression graphs; and Figure S8: the principal component (PC) plots (PDF)

■ AUTHOR INFORMATION

Corresponding Authors

Rafal Szmigielski − *Institute of Physical Chemistry, Polish Academy of Sciences, 01-224 Warsaw, Poland;* orcid.org/0000-0003-3389-9318; Email: ralf@ichf.edu.pl

Rebecca C. Fry − *Department of Environmental Sciences and Engineering, Gillings School of Global Public Health, University of North Carolina at Chapel Hill, Chapel Hill, North Carolina 27599, United States;* orcid.org/0000-0003-0899-9018; Email: rfry@unc.edu

Jason D. Surratt − *Department of Environmental Sciences and Engineering, Gillings School of Global Public Health and Department of Chemistry, University of North Carolina at Chapel Hill, Chapel Hill, North Carolina 27599, United States;* orcid.org/0000-0002-6833-1450; Email: surratt@unc.edu

Authors

Faria Khan − *Institute of Physical Chemistry, Polish Academy of Sciences, 01-224 Warsaw, Poland; Department of Environmental Sciences and Engineering, Gillings School of Global Public Health, University of North Carolina at Chapel Hill, Chapel Hill, North Carolina 27599, United States;* orcid.org/0000-0001-6539-888X

Yuzhi Chen − *Department of Environmental Sciences and Engineering, Gillings School of Global Public Health, University of North Carolina at Chapel Hill, Chapel Hill, North Carolina 27599, United States;* orcid.org/0000-0002-2547-8428

Hadley J. Hartwell − *Department of Environmental Sciences and Engineering, Gillings School of Global Public Health, University of North Carolina at Chapel Hill, Chapel Hill, North Carolina 27599, United States;* orcid.org/0000-0003-4453-3266

Jin Yan − *Department of Environmental Sciences and Engineering, Gillings School of Global Public Health, University of North Carolina at Chapel Hill, Chapel Hill, North Carolina 27599, United States*

Ying-Hsuan Lin − *Department of Environmental Sciences, University of California, Riverside, California 92521, United States;* orcid.org/0000-0001-8904-1287

Anastasia Freedman − *Department of Environmental Sciences and Engineering, Gillings School of Global Public Health, University of North Carolina at Chapel Hill, Chapel Hill, North Carolina 27599, United States*

Zhenfa Zhang − *Department of Environmental Sciences and Engineering, Gillings School of Global Public Health, University of North Carolina at Chapel Hill, Chapel Hill, North Carolina 27599, United States*

Yue Zhang − *Department of Environmental Sciences and Engineering, Gillings School of Global Public Health, University of North Carolina at Chapel Hill, Chapel Hill, North Carolina 27599, United States; Department of*

https://doi.org/10.1021/acs.chemrestox.3c00278
Chem. Res. Toxicol. XXXX, XXX, XXX−XXX

Atmospheric Sciences, Texas A&M University, College Station, Texas 77843, United States

Andrew T. Lambe − *Aerodyne Research Inc, Billerica, Massachusetts 01821, United States;* orcid.org/0000-0003-3031-701X

Barbara J. Turpin − *Department of Environmental Sciences and Engineering, Gillings School of Global Public Health, University of North Carolina at Chapel Hill, Chapel Hill, North Carolina 27599, United States;* orcid.org/0000-0003-4513-4187

Avram Gold − *Department of Environmental Sciences and Engineering, Gillings School of Global Public Health, University of North Carolina at Chapel Hill, Chapel Hill, North Carolina 27599, United States;* orcid.org/0000-0003-1383-6635

Andrew P. Ault − *Department of Chemistry, College of Literature, Science, and the Arts, University of Michigan, Ann Arbor, Michigan 48109, United States;* orcid.org/0000-0002-7313-8559

Complete contact information is available at: https://pubs.acs.org/10.1021/acs.chemrestox.3c00278

Author Contributions

CRediT: **FARIA KHAN** conceptualization, formal analysis, investigation, methodology, writing-original draft, writing-review & editing; **Yuzhi Chen** formal analysis, investigation, methodology, writing-review & editing; **Hadley J Hartwell** formal analysis, investigation, methodology, writing-review & editing; **Barbara J. Turpin** writing-review & editing; **Jin Yan** formal analysis, investigation, methodology, writing-review & editing; **Ying-Hsuan Lin** formal analysis, investigation, methodology, writing-review & editing; **Anastasia Freedman** methodology, writing-review & editing; **Zhenfa Zhang** synthesis of 2-MTS and other organic standards, writing-review & editing; **Yue Zhang** formal analysis, investigation, methodology, writing-review & editing; **Andrew T. Lambe** investigation, methodology, formal analysis, writing-review & editing; **Avram Gold** synthesis of 2-MTS and other organic standards, investigation, methodology, writing-review & editing; **Andrew P. Ault** writing-review & editing; **Rafal Szmigielski** conceptualization, funding acquisition, project administration, resources, supervision, validation, writing-original draft, writing-review & editing; **Rebecca C. Fry** conceptualization, funding acquisition, resources, supervision, writing-review & editing; **Jason D. Surratt** conceptualization, funding acquisition, methodology, project administration, resources, supervision, validation, writing-original draft, writing-review & editing.

Funding

Research reported in this publication was supported by the National Institutes of Health (NIH), specifically the National Institute of Environmental Health Sciences (NIEHS) (P30ES010126). F.K. and R.S. would like to acknowledge the funding support of the European Union's Horizon 2020 research and innovation program under the Marie Skłodowska-Curie grant agreement No. 711859 and by financial resources for science in the years 2017−2021 awarded by the Polish Ministry of Science and Higher Education for the implementation of an international cofinanced project. J.D.S., A.P.A., Y.C., J.Y., Y.Z., Z.Z., and A.G. were supported in part by funding from the National Science Foundation (NSF), including from Grant Nos. AGS-1703535, AGS-2039788, AGS-1703019, AGS-2040610, and AGS-2001027. Y.Z. was supported in part by funding from NSF AGS-PRF-1524731.

Notes

The authors declare no competing financial interest.

■ REFERENCES

(1) Wang, J. L.; Zhang, Y. H.; Shao, M.; Liu, X. L.; Zeng, L. M.; Cheng, C. L.; Xu, X. F. Quantitative relationship between visibility and mass concentration of PM2.5 in Beijing. *J. Environ. Sci. (China)* **2006**, *18* (3), 475−481.

(2) Requia, W. J.; Jhun, I.; Coull, B. A.; Koutrakis, P. Climate impact on ambient PM2.5 elemental concentration in the United States: A trend analysis over the last years. *Environ. Int.* **2019**, *131*, 104888.

(3) Xing, Y.-F.; Xu, Y.-H.; Shi, M.-H.; Lian, Y.-X. The impact of PM2.5 on the human respiratory system. *J. Thorac. Dis* **2016**, *8* (1), E69−E74.

(4) Xu, D.; Chen, Y.; Wu, L.; He, S.; Xu, P.; Zhang, Y.; Luo, J.; Ye, X.; Chen, Z.; Wang, X.; et al. Acute effects of ambient PM2.5 on lung function among schoolchildren. *Sci. Rep.* **2020**, *10* (1), 4061.

(5) Li, R.; Zhou, R.; Zhang, J. Function of PM2.5 in the pathogenesis of lung cancer and chronic airway inflammatory diseases. *Oncol. Lett.* **2018**, *15* (5), 7506−7514.

(6) Meier, R.; Cascio, W. E.; Ghio, A. J.; Wild, P.; Danuser, B.; Riediker, M. Associations of short-term particle and noise exposures with markers of cardiovascular and respiratory health among highway maintenance workers. *Environ. Health Perspect.* **2014**, *122* (7), 726−732. Huang, W.; Wang, G.; Lu, S. E.; Kipen, H.; Wang, Y.; Hu, M.; Lin, W.; Rich, D.; Ohman-Strickland, P.; Diehl, S. R.; et al. Inflammatory and oxidative stress responses of healthy young adults to changes in air quality during the Beijing Olympics. *Am. J. Respir Crit. Care Med.* **2012**, *186* (11), 1150−1159.

(7) Van Eeden, S. F.; Tan, W. C.; Suwa, T.; Mukae, H.; Terashima, T.; Fujii, T.; Qui, D.; Vincent, R.; Hogg, J. C. Cytokines involved in the systemic inflammatory response induced by exposure to particulate matter air pollutants (PM10). *Am. J. Respir. Crit. Care Med.* **2001**, *164* (5), 826−830.

(8) Wang, J.; Tang, B.; Liu, X.; Wu, X.; Wang, H.; Xu, D.; Guo, Y. Increased monomeric CRP levels in acute myocardial infarction: a possible new and specific biomarker for diagnosis and severity assessment of disease. *Atherosclerosis* **2015**, *239* (2), 343−349.

(9) Du, Y.; Xu, X.; Chu, M.; Guo, Y.; Wang, J. Air particulate matter and cardiovascular disease: the epidemiological, biomedical and clinical evidence. *J. Thorac. Dis.* **2016**, *8* (1), E8−E19. PubMed

(10) Martinelli, N.; Olivieri, O.; Girelli, D. Air particulate matter and cardiovascular disease: a narrative review. *Eur. J. Intern. Med.* **2013**, *24* (4), 295−302. Chan, S. H.; Van Hee, V. C.; Bergen, S.; Szpiro, A. A.; DeRoo, L. A.; London, S. J.; Marshall, J. D.; Kaufman, J. D.; Sandler, D. P. Long-Term Air Pollution Exposure and Blood Pressure in the Sister Study. *Environ. Health Perspect.* **2015**, *123* (10), 951−958.

(11) Hallquist, M.; Wenger, J. C.; Baltensperger, U.; Rudich, Y.; Simpson, D.; Claeys, M.; Dommen, J.; Donahue, N.; George, C.; Goldstein, A. The formation, properties and impact of secondary organic aerosol: current and emerging issues. *Atmos. Chem. Phys.* **2009**, *9* (14), 5155−5236.

(12) Guenther, A.; Karl, T.; Harley, P.; Wiedinmyer, C.; Palmer, P.; Geron, C. Estimates of global terrestrial isoprene emissions using MEGAN (Model of Emissions of Gases and Aerosols from Nature) *Atmos. Chem. Phys.* 2006, *6*, 3181−3210, DOI: 10.5194/acp-6-3181-2006. Guenther, A. B.; Jiang, X.; Heald, C. L.; Sakulyanontvittaya, T.; Duhl, T.; Emmons, L. K.; Wang, X. The Model of Emissions of Gases and Aerosols from Nature version 2.1 (MEGAN2.1): an extended and updated framework for modeling biogenic emissions. *Geosci. Model Dev.* **2012**, *5* (6), 1471−1492.

(13) St Clair, J. M.; Rivera-Rios, J. C.; Crounse, J. D.; Knap, H. C.; Bates, K. H.; Teng, A. P.; JĆørgensen, S.; Kjaergaard, H. G.; Keutsch, F. N.; Wennberg, P. O. Kinetics and Products of the Reaction of the First-Generation Isoprene Hydroxy Hydroperoxide (ISOPOOH) with OH. *J. Phys. Chem. A* **2016**, *120* (9), 1441−1451.

(14) Riva, M.; Budisulistiorini, S. H.; Chen, Y.; Zhang, Z.; D'Ambro, E. L.; Zhang, X.; Gold, A.; Turpin, B. J.; Thornton, J. A.; Canagaratna, M. R.; et al. Chemical Characterization of Secondary Organic Aerosol from Oxidation of Isoprene Hydroxyhydroperoxides. *Environ. Sci. Technol.* **2016**, *50* (18), 9889−9899. Claeys, M.; Graham, B.; Vas, G.; Wang, W.; Vermeylen, R.; Pashynska, V.; Cafmeyer, J.; Guyon, P.; Andreae, M. O.; Artaxo, P. Formation of secondary organic aerosols through photooxidation of isoprene. *Science* **2004**, *303* (5661), 1173−1176. Surratt, J. D.; Chan, A. W. H.; Eddingsaas, N. C.; Chan, M.; Loza, C. L.; Kwan, A. J.; Hersey, S. P.; Flagan, R. C.; Wennberg, P. O.; Seinfeld, J. H. Reactive intermediates revealed in secondary organic aerosol formation from isoprene. *Proc. Natl. Acad. Sci. U. S. A.* **2010**, *107* (15), 6640−6645. Surratt, J. D.; Murphy, S. M.; Kroll, J. H.; Ng, N. L.; Hildebrandt, L.; Sorooshian, A.; Szmigielski, R.; Vermeylen, R.; Maenhaut, W.; Claeys, M. Chemical composition of secondary organic aerosol formed from the photooxidation of isoprene. *J. Phys. Chem. A* **2006**, *110* (31), 9665−9690.
(15) Budisulistiorini, S. H.; Baumann, K.; Edgerton, E. S.; Bairai, S. T.; Mueller, S.; Shaw, S. L.; Knipping, E. M.; Gold, A.; Surratt, J. D. Seasonal characterization of submicron aerosol chemical composition and organic aerosol sources in the southeastern United States: Atlanta, Georgia, and Look Rock, Tennessee. *Atmos. Chem. Phys.* **2016**, *16* (8), 5171−5189. Xu, L.; Guo, H.; Boyd, C. M.; Klein, M.; Bougiatioti, A.; Cerully, K. M.; Hite, J. R.; Isaacman-VanWertz, G.; Kreisberg, N. M.; Knote, C. Effects of anthropogenic emissions on aerosol formation from isoprene and monoterpenes in the southeastern United States. *Proc. Natl. Acad. Sci. U. S. A.* **2015**, *112* (1), 37−42.
(16) Glasius, M.; Bering, M. S.; Yee, L. D.; De Sc, S. S.; Isaacman VanWertz, G.; Wernis, R. A.; Barbosa, H. M. J.; Alexander, M. L.; Palm, B. B.; Hu, W.; et al. Organosulfates in aerosols downwind of an urban region in central Amazon. *Environ. Sci.: Processes Impacts* **2018**, *20* (11), 1546−1558.
(17) Cui, T.; Zeng, Z.; dos Santos, E. O.; Zhang, Z.; Chen, Y.; Zhang, Y.; Rose, C. A.; Budisulistiorini, S. H.; Collins, L. B.; Bodnar, W. M.; et al. Development of a hydrophilic interaction liquid chromatography (HILIC) method for the chemical characterization of water-soluble isoprene epoxydiol (IEPOX)-derived secondary organic aerosol. *Environ. Sci.: Processes Impacts* **2018**, *20* (11), 1524−1536.
(18) Brüggemann, M.; Xu, R.; Tilgner, A.; Kwong, K. C.; Mutzel, A.; Poon, H. Y.; Otto, T.; Schaefer, T.; Poulain, L.; Chan, M. N.; et al. Organosulfates in Ambient Aerosol: State of Knowledge and Future Research Directions on Formation, Abundance, Fate, and Importance. *Environ. Sci. Technol.* **2020**, *54* (7), 3767−3782.
(19) Hettiyadura, A. P. S.; Stone, E. A.; Kundu, S.; Baker, Z.; Geddes, E.; Richards, K.; Humphry, T. Determination of atmospheric organosulfates using HILIC chromatography with MS detection. *Atmos. Meas. Tech.* **2015**, *8* (6), 2347−2358. Hughes, D. D.; Christiansen, M. B.; Milani, A.; Vermeuel, M. P.; Novak, G. A.; Alwe, H. D.; Dickens, A. F.; Pierce, R. B.; Millet, D. B.; Bertram, T. H.; Stanier, C. O.; Stone, E. A.; et al. PM2.5 chemistry, organosulfates, and secondary organic aerosol during the 2017 Lake Michigan Ozone Study. *Atmos. Environ.* **2021**, *244*, No. 117939.
(20) Chen, Y.; Zhang, Y.; Lambe, A. T.; Xu, R.; Lei, Z.; Olson, N. E.; Zhang, Z.; Szalkowski, T.; Cui, T.; Vizuete, W. Heterogeneous hydroxyl radical oxidation of isoprene-epoxydiol-derived methyltetrol sulfates: plausible formation mechanisms of previously unexplained organosulfates in ambient fine aerosols. *Environ. Sci. Technol. Lett.* **2020**, *7* (7), 460−468.
(21) Riva, M.; Chen, Y.; Zhang, Y.; Lei, Z.; Olson, N. E.; Boyer, H. C.; Narayan, S.; Yee, L. D.; Green, H. S.; Cui, T.; et al. Increasing Isoprene Epoxydiol-to-Inorganic Sulfate Aerosol Ratio Results in Extensive Conversion of Inorganic Sulfate to Organosulfur Forms: Implications for Aerosol Physicochemical Properties. *Environ. Sci. Technol.* **2019**, *53* (15), 8682−8694.
(22) Tiiva, P.; Faubert, P.; Michelsen, A.; Holopainen, T.; Holopainen, J. K.; Rinnan, R. Climatic warming increases isoprene emission from a subarctic heath. *New Phytol.* **2008**, *180* (4), 853−863. Turner, D. P.; Baglio, J. V.; Wones, A. G.; Pross, D.; Vong, R.; McVeety, B. D.; Phillips, D. L. Climate change and isoprene emissions from vegetation. *Chemosphere* **1991**, *23* (1), 37−56.
(23) Suratt, J. D.; Lin, Y.-H.; Arashiro, M.; Vizuete, W. G.; Zhang, Z.; Gold, A.; Jaspers, I.; Fry, R. C. Understanding the Early Biological Effects of Isoprene-Derived Particulate Matter Enhanced by Anthropogenic Pollutants. *Re. Rep. Health Eff. Inst.* **2019**, *2019*, 198.
(24) Arashiro, M.; Lin, Y. H.; Sexton, K. G.; Zhang, Z.; Jaspers, I.; Fry, R. C.; Vizuete, W. G.; Gold, A.; Surratt, J. D. In vitro exposure to isoprene-derived secondary organic aerosol by direct deposition and its effects on COX-2 and IL-8 gene expression. *Atmos. Chem. Phys.* **2016**, *16* (22), 14079−14090.
(25) Lin, Y. H.; Arashiro, M.; Clapp, P. W.; Cui, T.; Sexton, K. G.; Vizuete, W.; Gold, A.; Jaspers, I.; Fry, R. C.; Surratt, J. D. Gene Expression Profiling in Human Lung Cells Exposed to Isoprene-Derived Secondary Organic Aerosol. *Environ. Sci. Technol.* **2017**, *51* (14), 8166−8175.
(26) Rohr, A. C.; Shore, S. A.; Spengler, J. D. Repeated exposure to isoprene oxidation products causes enhanced respiratory tract effects in multiple murine strains. *Inhal. Toxicol.* **2003**, *15* (12), 1191−1207. Wilkins, C. K.; Clausen, P. A.; Wolkoff, P.; Larsen, S. T.; Hammer, M.; Larsen, K.; Hansen, V.; Nielsen, G. D. Formation of strong airway irritants in mixtures of isoprene/ozone and isoprene/ozone/nitrogen dioxide. *Environ. Health Perspect.* **2001**, *109* (9), 937−941.
(27) Wilkins, C. K.; Wolkoff, P.; Clausen, P. A.; Hammer, M.; Nielsen, G. D. Upper airway irritation of terpene/ozone oxidation products (TOPS). Dependence on reaction time, relative humidity and initial ozone concentration. *Toxicol. Lett.* **2003**, *143* (2), 109−114.
(28) Kramer, A. J.; Rattanavaraha, W.; Zhang, Z.; Gold, A.; Surratt, J. D.; Lin, Y.-H. Assessing the oxidative potential of isoprene-derived epoxides and secondary organic aerosol. *Atmos. Environ.* **2016**, *130*, 211−218.
(29) Doyle, M.; Sexton Kenneth, G.; Jeffries, H.; Bridge, K.; Jaspers, I. Effects of 1,3-Butadiene, Isoprene, and Their Photochemical Degradation Products on Human Lung Cells. *Environ. Health Perspect.* **2004**, *112* (15), 1488−1495. (acccessed 2021/08/31)
(30) Lin, Y.-H.; Arashiro, M.; Martin, E.; Chen, Y.; Zhang, Z.; Sexton, K. G.; Gold, A.; Jaspers, I.; Fry, R. C.; Surratt, J. D. Isoprene-derived secondary organic aerosol induces the expression of oxidative stress response genes in human lung cells. *Environ. Sci. Technol. Lett.* **2016**, *3* (6), 250−254.
(31) Arashiro, M.; Lin, Y.-H.; Zhang, Z.; Sexton, K. G.; Gold, A.; Jaspers, I.; Fry, R. C.; Surratt, J. D. Effect of secondary organic aerosol from isoprene-derived hydroxyhydroperoxides on the expression of oxidative stress response genes in human bronchial epithelial cells. *Environ. Sci.: Processes Impacts* **2018**, *20* (2), 332−339.
(32) Eaves, L. A.; Smeester, L.; Hartwell, H. J.; Lin, Y.-H.; Arashiro, M.; Zhang, Z.; Gold, A.; Surratt, J. D.; Fry, R. C. Isoprene-Derived Secondary Organic Aerosol Induces the Expression of MicroRNAs Associated with Inflammatory/Oxidative Stress Response in Lung Cells. *Chem. Res. Toxicol.* **2020**, *33* (2), 381−387.
(33) Alpert, P. A.; Dou, J.; Corral Arroyo, P.; Schneider, F.; Xto, J.; Luo, B.; Peter, T.; Huthwelker, T.; Borca, C. N.; Henzler, K. D.; et al. Photolytic radical persistence due to anoxia in viscous aerosol particles. *Nat. Commun.* **2021**, *12* (1), 1769.
(34) Hettiyadura, A. P. S.; Al-Naiema, I. M.; Hughes, D. D.; Fang, T.; Stone, E. A. Organosulfates in Atlanta, Georgia: anthropogenic influences on biogenic secondary organic aerosol formation. *Atmos. Chem. Phys.* **2019**, *19* (5), 3191−3206.
(35) Tomaz, S.; Cui, T.; Chen, Y.; Sexton, K. G.; Roberts, J. M.; Warneke, C.; Yokelson, R. J.; Surratt, J. D.; Turpin, B. J. Photochemical cloud processing of primary wildfire emissions as a potential source of secondary organic aerosol. *Environ. Sci. Technol.* **2018**, *52* (19), 11027−11037.
(36) Livak, K. J.; Schmittgen, T. D. Analysis of relative gene expression data using real-time quantitative PCR and the 2(-Delta Delta C(T)) Method. *Methods* **2001**, *25* (4), 402−408.

https://doi.org/10.1021/acs.chemrestox.3c00278
Chem. Res. Toxicol. XXXX, XXX, XXX−XXX

(37) Chen, Y.; Dombek, T.; Hand, J.; Zhang, Z.; Gold, A.; Ault, A. P.; Levine, K. E.; Surratt, J. D. Seasonal Contribution of Isoprene-Derived Organosulfates to Total Water-Soluble Fine Particulate Organic Sulfur in the United States. *ACS Earth Space Chem.* **2021**, *5*, 2419.

(38) Turpin, B. J.; Lim, H.-J. Species Contributions to PM2.5 Mass Concentrations: Revisiting Common Assumptions for Estimating Organic Mass. *Aerosol Sci. Technol.* **2001**, *35* (1), 602–610. Nakao, S.; Tang, P.; Tang, X.; Clark, C. H.; Qi, L.; Seo, E.; Asa-Awuku, A.; Cocker, D. Density and elemental ratios of secondary organic aerosol: Application of a density prediction method. *Atmos. Environ.* **2013**, *68*, 273–277.

(39) Budisulistiorini, S.; Li, X.; Bairai, S. T.; Renfro, J.; Liu, Y.; Liu, Y. J.; McKinney, K. A.; Martin, S. T.; McNeill, V. F.; Pye, H. O. T. Examining the effects of anthropogenic emissions on isoprene-derived secondary organic aerosol formation during the 2013 Southern Oxidant and Aerosol Study (SOAS) at the Look Rock, Tennessee ground site. *Atmos. Chem. Phys.* **2015**, *15* (15), 8871–8888. Rattanavaraha, W.; Chu, K.; Budisulistiorini, S. H.; Riva, M.; Lin, Y.-H.; Edgerton, E. S.; Baumann, K.; Shaw, S. L.; Guo, H.; King, L. Assessing the impact of anthropogenic pollution on isoprene-derived secondary organic aerosol formation in PM 2.5 collected from the Birmingham, Alabama, ground site during the 2013 Southern Oxidant and Aerosol Study. *Atmos. Chem. Phys.* **2016**, *16* (8), 4897–4914.

(40) Khan, F.; Kwapiszewska, K.; Zhang, Y.; Chen, Y.; Lambe, A. T.; Kołodziejczyk, A.; Jalal, N.; Rudzinski, K.; Martínez-Romero, A.; Fry, R. C.; et al. Toxicological Responses of α-Pinene-Derived Secondary Organic Aerosol and Its Molecular Tracers in Human Lung Cell Lines. *Chem. Res. Toxicol.* **2021**, *34* (3), 817–832.

(41) Chowdhury, P. H.; He, Q.; Lasitza Male, T.; Brune, W. H.; Rudich, Y.; Pardo, M. Exposure of Lung Epithelial Cells to Photochemically Aged Secondary Organic Aerosol Shows Increased Toxic Effects. *Environ. Sci. Technol. Lett.* **2018**, *5* (7), 424–430. Chowdhury, P. H.; He, Q.; Carmieli, R.; Li, C.; Rudich, Y.; Pardo, M. Connecting the Oxidative Potential of Secondary Organic Aerosols with Reactive Oxygen Species in Exposed Lung Cells. *Environ. Sci. Technol.* **2019**, *53* (23), 13949–13958.

(42) Han, J.; Wang, S.; Yeung, K.; Yang, D.; Gu, W.; Ma, Z.; Sun, J.; Wang, X.; Chow, C.-W.; Chan, A. W. H.; et al. Proteome-wide effects of naphthalene-derived secondary organic aerosol in BEAS-2B cells are caused by short-lived unsaturated carbonyls. *Proc. Natl. Acad. Sci. U. S. A.* **2020**, *117* (41), 25386.

(43) Cuadrado, A.; Manda, G.; Hassan, A.; Alcaraz, M. J.; Barbas, C.; Daiber, A.; Ghezzi, P.; León, R.; López, M. G.; Oliva, B. Transcription factor NRF2 as a therapeutic target for chronic diseases: a systems medicine approach. *Pharmacol. Rev.* **2018**, *70* (2), 348–383.

(44) Cuadrado, A.; Rojo, A. I.; Wells, G.; Hayes, J. D.; Cousin, S. P.; Rumsey, W. L.; Attucks, O. C.; Franklin, S.; Levonen, A.-L.; Kensler, T. W.; et al. Therapeutic targeting of the NRF2 and KEAP1 partnership in chronic diseases. *Nat. Rev. Drug Discov.* **2019**, *18* (4), 295–317.

(45) Biswas, S. K.; Rahman, I. Environmental toxicity, redox signaling and lung inflammation: The role of glutathione. *Mol. Asp. Med.* **2009**, *30* (1), 60–76.

(46) Ralat, L. A.; Manevich, Y.; Fisher, A. B.; Colman, R. F. Direct evidence for the formation of a complex between 1-cysteine peroxiredoxin and glutathione S-transferase π with activity changes in both enzymes. *Biochemistry* **2006**, *45* (2), 360–372.

(47) Choi, J.; Liu, R.-M.; Kundu, R. K.; Sangiorgi, F.; Wu, W.; Maxson, R.; Forman, H. J. Molecular mechanism of decreased glutathione content in human immunodeficiency virus type 1 Tat-transgenic mice. *J. Biol. Chem.* **2000**, *275* (5), 3693–3698.

(48) Fletcher, M. E.; Boshier, P. R.; Wakabayashi, K.; Keun, H. C.; Smolenski, R. T.; Kirkham, P. A.; Adcock, I. M.; Barton, P. J.; Takata, M.; Marczin, N. Influence of glutathione-S-transferase (GST) inhibition on lung epithelial cell injury: role of oxidative stress and metabolism. *Am. J. Physiol.-Lung Cell. Mol. Physiol.* **2015**, *308* (12), L1274–L1285. (acccessed 2021/08/20)

(49) Carlberg, I.; Mannervik, B. [59] Glutathione reductase. *Methods Enzymol.* **1985**, *113*, 484–490.

(50) Zelko, I. N.; Mariani, T. J.; Folz, R. J. Superoxide dismutase multigene family: a comparison of the CuZn-SOD (SOD1), Mn-SOD (SOD2), and EC-SOD (SOD3) gene structures, evolution, and expression. *Free Radic. Biol. Med.* **2002**, *33* (3), 337–349.

(51) Vignais, P. V. The superoxide-generating NADPH oxidase: structural aspects and activation mechanism. *Cell. Mol. Life Sci.* **2002**, *59* (9), 1428–1459.

(52) Aris, R. M.; Christian, D.; Hearne, P. Q.; Kerr, K.; Finkbeiner, W. E.; Balmes, J. R. Ozone-induced airway inflammation in human subjects as determined by airway lavage and biopsy. *Am. Rev. Respir. Dis.* **1993**, *148* (5), 1363–1372.

(53) Bromberg, P. A. Mechanisms of the acute effects of inhaled ozone in humans. *Biochim. Biophys. Acta-Gen. Subj.* **2016**, *1860* (12), 2771–2781.

(54) Islam, T.; McConnell, R.; Gauderman, W. J.; Avol, E.; Peters, J. M.; Gilliland, F. D. Ozone, Oxidant Defense Genes, and Risk of Asthma during Adolescence. *Am. J. Respir. Crit. Care Med.* **2008**, *177* (4), 388–395. Exner, M.; Minar, E.; Wagner, O.; Schillinger, M. The role of heme oxygenase-1 promoter polymorphisms in human disease. *Free Radic. Biol. Med.* **2004**, *37* (8), 1097–1104.

(55) Borish, L. IL-10: Evolving concepts. *J. Allergy Clin. Immunol.* **1998**, *101* (3), 293–297.

(56) Badran, G.; Verdin, A.; Grare, C.; Abbas, I.; Achour, D.; Ledoux, F.; Roumie, M.; Cazier, F.; Courcot, D.; Lo Guidice, J. M.; Garçon, G.; et al. Toxicological appraisal of the chemical fractions of ambient fine (PM2.5–0.3) and quasi-ultrafine (PM0.3) particles in human bronchial epithelial BEAS-2B cells. *Environ. Pollut.* **2020**, *263*, No. 114620.

(57) Frias, D. P.; Gomes, R. L. N.; Yoshizaki, K.; Carvalho-Oliveira, R.; Matsuda, M.; Junqueira, M. S.; Teodoro, W. R.; Vasconcellos, P. C.; Pereira, D. C. A.; Conceição, P. R. D.; et al. Nrf2 positively regulates autophagy antioxidant response in human bronchial epithelial cells exposed to diesel exhaust particles. *Sci. Rep* **2020**, *10* (1), 3704. Ito, T.; Bekki, K.; Fujitani, Y.; Hirano, S. The toxicological analysis of secondary organic aerosol in human lung epithelial cells and macrophages. *Environ. Sci. Pollut. Res.* **2019**, *26* (22), 22747–22755. Merk, R.; Heßelbach, K.; Osipova, A.; Popadić, D.; Schmidt-Heck, W.; Kim, G.-J.; Günther, S.; Piñeres, A. G.; Merfort, I.; Humar, M. Particulate Matter (PM2.5) from Biomass Combustion Induces an Anti-Oxidative Response and Cancer Drug Resistance in Human Bronchial Epithelial BEAS-2B Cells. *Int. J. Environ. Res. Public Health* **2020**, *17* (21), 8193.

(58) Dhakshinamoorthy, S.; Long 2nd, D. J.; Jaiswal, A. K. Antioxidant regulation of genes encoding enzymes that detoxify xenobiotics and carcinogens. *Curr. Top. Cell Regul.* **2000**, *36*, 201–216.

(59) Niture, S. K.; Kaspar, J. W.; Shen, J.; Jaiswal, A. K. Nrf2 signaling and cell survival. *Toxicol. Appl. Pharmacol.* **2010**, *244* (1), 37–42. PubMed

(60) Kinnula, V. L.; Crapo, J. D. Superoxide dismutases in the lung and human lung diseases. *Am. J. Respir Crit Care Med.* **2003**, *167* (12), 1600–1619.

(61) Bernard, K.; Hecker, L.; Luckhardt, T. R.; Cheng, G.; Thannickal, V. J. NADPH Oxidases in Lung Health and Disease. *Antioxid. Redox Signal.* **2013**, *20* (17), 2838–2853. (acccessed 2021/08/25)

(62) Betsuyaku, T.; Fuke, S.; Inomata, T.; Kaga, K.; Morikawa, T.; Odajima, N.; Adair-Kirk, T.; Nishimura, M. Bronchiolar epithelial catalase is diminished in smokers with mild COPD. *Eur. Respir. J.* **2013**, *42* (1), 42.

(63) Guan, S. P.; Tee, W.; Ng, D. S. W.; Chan, T. K.; Peh, H. Y.; Ho, W. E.; Cheng, C.; Mak, J. C.; Wong, W. S. F. Andrographolide protects against cigarette smoke-induced oxidative lung injury via augmentation of Nrf2 activity. *Br. J. Pharmacol.* **2013**, *168* (7), 1707–1718.

(64) Otterbein, L. E.; Soares, M. P.; Yamashita, K.; Bach, F. H. Heme oxygenase-1: unleashing the protective properties of heme. *Trends Immunol.* **2003**, *24* (8), 449−455.

(65) Harju, T.; Soini, Y.; Pääkkö, R.; Kinnula, V. L. Up-regulation of heme oxygenase-I in alveolar macrophages of newly diagnosed asthmatics. *Respir. Med.* **2002**, *96* (6), 418−423.

(66) Fredenburgh, L. E.; Perrella, M. A.; Mitsialis, S. A. The role of heme oxygenase-1 in pulmonary disease. *Am. J. Respir. Cell Mol. Biol.* **2007**, *36* (2), 158−165. PubMed

(67) Weldy, C. S.; White, C. C.; Wilkerson, H.-W.; Larson, T. V.; Stewart, J. A.; Gill, S. E.; Parks, W. C.; Kavanagh, T. J. Heterozygosity in the glutathione synthesis gene Gclm increases sensitivity to diesel exhaust particulate induced lung inflammation in mice. *Inhal. Toxicol.* **2011**, *23* (12), 724−735. McConnachie, L. A.; Botta, D.; White, C. C.; Weldy, C. S.; Wilkerson, H. W.; Yu, J.; Dills, R.; Yu, X.; Griffith, W. C.; Faustman, E. M.; Farin, F. M.; Gill, S. E.; Parks, W. C.; Hu, X.; Gao, X.; Eaton, D. L.; Kavanagh, T. J.; Rogers, L. K.; et al. The Glutathione Synthesis Gene Gclm Modulates Amphiphilic Polymer-Coated CdSe/ZnS Quantum Dot-Induced Lung Inflammation in Mice. *PLoS One* **2013**, *8* (5), No. e64165.

(68) van der Toorn, M.; Smit-de Vries, M. P.; Slebos, D. J.; de Bruin, H. G.; Abello, N.; van Oosterhout, A. J.; Bischoff, R.; Kauffman, H. F. Cigarette smoke irreversibly modifies glutathione in airway epithelial cells. *Am. J. Physiol. Lung Cell. Mol. Physiol.* **2007**, *293* (5), L1156−1162.

(69) Ahmed, C. M. S.; Yang, J.; Chen, J. Y.; Jiang, H.; Cullen, C.; Karavalakis, G.; Lin, Y. H. Toxicological responses in human airway epithelial cells (BEAS-2B) exposed to particulate matter emissions from gasoline fuels with varying aromatic and ethanol levels. *Sci. Total Environ.* **2020**, *706*, No. 135732.

(70) Bryant, D. J.; Dixon, W. J.; Hopkins, J. R.; Dunmore, R. E.; Pereira, K. L.; Shaw, M.; Squires, F. A.; Bannan, T. J.; Mehra, A.; Worrall, S. D.; et al. Strong anthropogenic control of secondary organic aerosol formation from isoprene in Beijing. *Atmos. Chem. Phys.* **2020**, *20* (12), 7531−7552.

(71) Kristiansen, N. I.; Stohl, A.; Olivié, D. J. L.; Croft, B.; Søvde, O. A.; Klein, H.; Christoudias, T.; Kunkel, D.; Leadbetter, S. J.; Lee, Y. H.; et al. Evaluation of observed and modelled aerosol lifetimes using radioactive tracers of opportunity and an ensemble of 19 global models. *Atmos. Chem. Phys.* **2016**, *16* (5), 3525−3561.

(72) Lu, K. D.; Hofzumahaus, A.; Holland, F.; Bohn, B.; Brauers, T.; Fuchs, H.; Hu, M.; Häseler, R.; Kita, K.; Kondo, Y.; et al. Missing OH source in a suburban environment near Beijing: observed and modelled OH and HO concentrations in summer 2006. *Atmos. Chem. Phys.* **2013**, *13* (2), 1057−1080. Ortega, A. M.; Hayes, P. L.; Peng, Z.; Palm, B. B.; Hu, W.; Day, D. A.; Li, R.; Cubison, M. J.; Brune, W. H.; Graus, M.; et al. Real-time measurements of secondary organic aerosol formation and aging from ambient air in an oxidation flow reactor in the Los Angeles area. *Atmos. Chem. Phys.* **2016**, *16* (11), 7411−7433.

(73) Khan, F.; Jaoui, M.; Rudziński, K.; Kwapiszewska, K.; Martinez-Romero, A.; Gil-Casanova, D.; Lewandowski, M.; Kleindienst, T. E.; Offenberg, J. H.; Krug, J. D.; Surratt, J. D.; Szmigielski, R.; et al. Cytotoxicity and oxidative stress induced by atmospheric mono-nitrophenols in human lung cells. *Environ. Pollut.* **2022**, *301*, No. 119010.

(74) Wilkins, C. K.; Wolkoff, P.; Clausen, P. A.; Hammer, M.; Nielsen, G. D. Upper airway irritation of terpene/ozone oxidation products (TOPS). Dependence on reaction time, relative humidity and initial ozone concentration. *Toxicol. Lett.* **2003**, *143* (2), 109−114. Rohr, A. C.; Wilkins, C. K.; Clausen, P. A.; Hammer, M.; Nielsen, G. D.; Wolkoff, P.; Spengler, J. D. Upper airway and pulmonary effects of oxidation products of (+)-alpha-pinene, d-limonene, and isoprene in BALB/c mice. *Inhal. Toxicol.* **2002**, *14* (7), 663−684.